BRIEF COMMUNICATION

Optical and Structural Investigation of KMgLa(PO$_4$)$_2$ Phosphate Doped with Europium

Shaolong Tie, Qiang Su,[1] and Yaqin Yu

Changchun Institute of Applied Chemistry, Chinese Academy of Science, Changchun 130022, People's Republic of China

A new compound KMgLa(PO$_4$)$_2$, isotypic with monoclinic LaPO$_4$, is reported. Its cell parameters have been determined from X-ray powder diffraction data. Crystallization occurs in the monoclinic space group $P2_1/n$ (No. 14) with $a = 6.839(3)$ Å, $b = 7.066(1)$ Å, $c = 6.523(3)$ Å, $\beta = 103.42(4)°$, and $Z = 2$. It was found that the KMgLa(PO$_4$)$_2$ phase was isostructural with monoclinic LaPO$_4$. The difference between them was that half of the La atoms in LaPO$_4$ were couplingly substituted with the same amount of Mg and K atoms. This isomorphous substitution was confirmed by IR and Eu^{3+}-doped excitation and emission spectra and by elemental analysis of single crystals. The spectroscopic data were compared with those of LaPO$_4$:Eu^{3+}. © 1995 Academic Press, Inc.

INTRODUCTION

In recent years, a series of double phosphates with general formula $ABLn$ (PO$_4$)$_2$ (A = alkali, B = alkaline earth, Ln = La–Lu and Y), isotypic with LaPO$_4$, have been reported. Most of them show a hexagonal structure (1, 2); a few of them belong to the monoclinic or tetragonal system (3). It seems that each double phosphate $ABLn$ (PO$_4$)$_2$ also possesses three allotropies, just like those of LnPO$_4$ (Ln = La–Gd). Our recent studies have confirmed this point of view. For $ABLn$ (PO$_4$)$_2$, the monoclinic phase forms at lower temperatures, and the hexagonal one mainly exists at higher temperatures.

It is worth noting that some of the monoclinic phases of $ABLn$ (PO$_4$)$_2$ doped with R^{3+} (R^{3+} = Eu^{3+}, Ce^{3+}, and Ce^{3+}–Tb^{3+}) exhibit strong luminescence under 254-nm excitation and could be used as trichromatic phosphors or for a special usage.

The crystal structure of monoclinic LnPO$_4$ (Ln = La and Ce) has been re-examined by Beall *et al.* (4) and Mullica *et al.* (5), respectively. Both demonstrated that the structure is isotypic with monazite. The Ln atom is ninefold coordinated with oxygen atoms and the LnO$_9$ polyhedron is non-regular, viz., an irregular pentagon with two oxygen atoms above and two oxygen atoms

[1] To whom correspondence should be addressed.

below the plane of the pentagon. The point symmetry for the Ln local site is Cs. As shown in Fig. 1, large channels along the c-axis exist in the monoclinic phase of LnPO$_4$. Our recent experimental results proved that half of the Ln^{3+} ions could be replaced simultaneously by B^{2+} and A^+ ions with no striking change in the crystal lattice. One is located at the site of Ln^{3+}; the other could be accommodated into the channels.

Herein, we report one of the analogues of monoclinic LnPO$_4$, e.g., KMgLa(PO$_4$)$_2$. Its IR absorption and Eu^{3+}-doped excitation and emission spectra are discussed in comparison with those of monoclinic LaPO$_4$ phase.

EXPERIMENTAL

The powder samples were obtained with a solid-state reaction from stoichiometric mixtures of potassium carbonate, magnesia (analytic grade), rare-earth oxides (4N-grade, Yuelong Co., Shanghai), and diammonium hydrogen phosphate (analytic grade). In order to get a single phase, an appropriate amount of flux and two firing steps were necessary, one at 200–400°C for 6 hr and the other at 880°C for several hours with interposed grinding. The LaPO$_4$ samples were synthesized based on Ref. (6).

The single crystals of KMgLa(PO$_4$)$_2$ were grown by the flux method. The mixture with KCl: KMgLa(PO$_4$)$_2$ ratio of 5:1 was melted in a platinum crucible at a suitable temperature, and then held overnight at 950°C. The temperature was reduced at 5°C/hr to 650°C, after which the furnace was turned off. The cooled material, which contained some needle-shaped crystals, was washed in cool water. The final crystals gave the same X-ray powder pattern and IR spectrum.

The X-ray powder diffraction data of KMgLa(PO$_4$)$_2$ were carried out with a Rigaku X-ray diffractometer (model D/max-II B) using single-crystal Si powder as an internal standard. The unit-cell parameters were calculated from a least-squares refinement of 20 stronger Cu$K\alpha_1$ reflection planes ($\lambda = 1.54056$ Å) collected between $2\theta = 10°$ and $2\theta = 60°$ at room temperature.
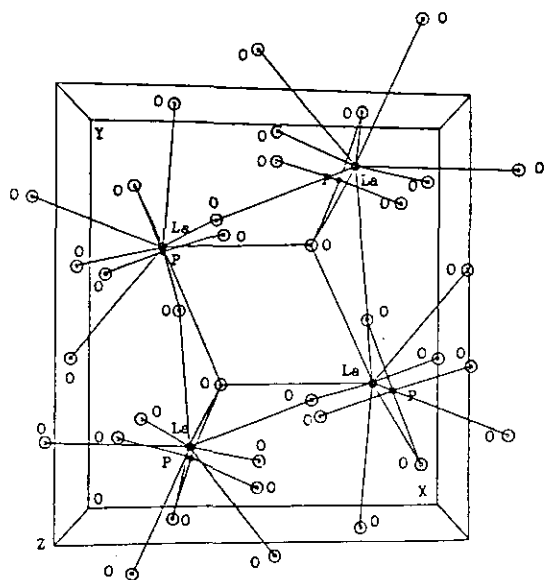
FIG. 1. Stereoscopic packing diagram for monoclinic LaPO₄.

powder is hygroscopic and partly hydrolyzes (pH > 8) in water.

Further information about the Mg^{2+} and K^+ positions will be reported in the future from the single-crystal data of $KMgLa(PO_4)_2$.

SPECTROSCOPIC PROPERTIES OF $KMgLa(PO_4)_2$

IR Spectra

IR spectra of $LnPO_4$ were studied in detail by Hezel and Ross (9). Structural differences between hydrous and anhydrous $LnPO_4$ can be distinguished by their IR spectra. For monoclinic forms of anhydrous $LnPO_4$ (Ln = La–Tb) with the Cs site symmetry of the PO_4 group, usually five or six bands appear in the ν_3 region and four in the ν_4 region, as shown in Table 2.

Our IR data for anhydrous $LaPO_4$ are in agreement with those of Hezel and Ross. The sample doped with Eu^{3+}

The emission and excitation spectra were measured at 300 K with a Hitachi fluorescence spectrophotometer (model M-850). The IR absorption spectra were obtained with a Perkin–Elmer infrared spectrophotometer, model 580B.

CRYSTAL STRUCTURE OF $KMgLa(PO_4)_2$

The elemental analysis for P and La in $KMgLa(PO_4)_2$ single crystals was carried out mainly based on Ref. (7). The AAS method was used to measure the K and Mg contents. Finally, we gained the following results (in weight percent): K 11. 78 (theoretical value 9.97), Mg 6.76 (6.20), La 34.80 (35.41), and P 15. 91 (15.79), respectively. On account of the errors from the method and our instrument of AAS (Model, P-E 403), the results for the K, Mg values seem higher to some degree than we expected. The values for La and P content, which are in good agreement with the formula $KMgLa(PO_4)_2$, however, prove that the single crystals we obtained really have the composition $KMgLa(PO_4)_2$.

The X-ray powder pattern of $KMgLa(PO_4)_2$ was very similar to that of $LaPO_4$ (JCPDF 12-285). The $d_{exp.}$, hkl, I/I_0, and $d_{calc.}$ are given in Table 1.

The crystal data calculated from the powder pattern of $KMgLa(PO_4)_2$ are a = 6.839(3) Å, b = 7.066(1) Å, c = 6.523(3) Å, β = 103.42(4)°, Z = 2, space group $P2_1/n$; D_x = 4.277(1), $D_{exp.}$ = 4.242(2), and V = 307 Å³. Its cell constants and unit-cell volume are comparable to those of monoclinic $LaPO_4$ (8). The powder density of $KMgLa(PO_4)_2$ was determined with a pycnometer using CCl_4 as a solvent instead of water, since the $KMgLa(PO_4)_2$

TABLE 1
X-Ray Powder Data for Lanthanum Magnesium Potassium Phosphate

$d_{exp.}$ (Å)	I/I_0	hkl	$d_{calc.}$ (Å)
5.223	10	$\bar{1}01$	5.2389
4.844	8	110	4.8436
4.721	17	011	4.7210
4.203	34	$\bar{1}11$	4.2084
4.141	14	101	4.1368
3.570	12	111	3.5700
3.533	17	020	3.5330
3.326	54	200	3.3262
3.186	13	002	3.1725
3.120	100	120	3.1203
3.011	15	210	3.0095
2.970	4	$\bar{2}11$	2.9715
2.887	74	$\bar{1}12$	2.8870
2.610	20	$\bar{2}02$	2.6195
2.467	8	112	2.4695
2.450	13	$\bar{2}12$	2.4561
2.423	6	220	2.4218
2.350	3	$\bar{1}22$	2.3566
2.208	19	031	2.2081
2.158	29	$\bar{3}11$	2.1555
1.985	26	212	1.9851
1.956	5	301	1.9566
1.911	10	$\bar{2}31$	1.9122
1.887	23	$\bar{1}32$	1.8891
1.812	7	023	1.8147
1.774	14	231	1.7748
1.756	16	132	1.7563
1.742	8	$\bar{2}23$	1.7459
1.708	8	140	1.7073
1.663	3	400	1.6631
1.634	4	$\bar{3}31$	1.6320
1.616	4	330	1.6145
1.604	3	312	1.6039

TABLE 2

Infrared Spectra of KMgLa(PO$_4$)$_2$ and LaPO$_4$ (in cm^{-1})

Symmetry	LaPO$_4$		LaPO$_4$		KMgLa(PO$_4$)$_2$	
	Cs		*Cs*		*Cs*	
ν_3	1087	1075 sh	1085	—	1086	1069 sh
	1053 sh	1025	1055	1020	—	1030
	1010	980	1010	986	1006	988
ν_1	946		947		948	
ν_4	621	575	612	572	617	572
	559	532	559	531	558	530
ν_2	487		498		494	
Ref.	(9)		This work		This work	

(La$_{0.94}$Eu$_{0.06}$PO$_4$) does not change its spectrum from LaPO$_4$.

From Table 2, it can be seen that the IR spectrum of KMgLa(PO$_4$)$_2$ is similar to that of LaPO$_4$. This confirms that the structure of KMgLa(PO$_4$)$_2$ is also monoclinic with *Cs* site symmetry like that of LaPO$_4$.

The IR spectrum of KMgLa$_{0.90}$Eu$_{0.10}$(PO$_4$)$_2$ looks like that of KMgLa(PO$_4$)$_2$. It seems more likely that isomorphous substitution between La^{3+} and Eu^{3+} can take place.

Emission and Excitation Spectra

As shown in Table 2 in the KMgLa(PO$_4$)$_2$ matrix, the vibrational energy of the P–O bond is high (ca. 1000 cm^{-1}), which means that only 2–3 phonons are needed to fill the energy gap of 2000 cm^{-1} between the $^5D_1$ and $^5D_0$ (as well as between the $^5D_2$ and $^5D_1$) levels. Such a process involving simultaneous absorption of 2–3 phonons is highly probable and thus explains why the $^5D_0 \rightarrow {}^7F_j$ emission of Eu^{3+} in KMgLa(PO$_4$)$_2$ and LaPO$_4$ is predominant, as demonstrated in Fig. 2. The emission spectrum for KMgLa(PO$_4$)$_2$: Eu^{3+} we observed is in agreement with that reported previously in Ref. (3) except for the $^5D_0-{}^7F_0$ transition. The corresponding wavelengths and energy levels of Eu^{3+} are listed in Table 3.

The number of observed emission lines (one for $^5D_0 \rightarrow {}^7F_0$, three for $^5D_0 \rightarrow {}^7F_1$, and five for $^5D_0 \rightarrow {}^7F_2$) indicates complete removal of ^7F_j degeneracies; this may correspond to a lower point symmetry of the rare earth site, e.g., *Cs*, in agreement with the result obtained by X-ray diffraction (5).

The $^7F_1$ and $^7F_2$ baricenters for KMgLa(PO$_4$)$_2$: Eu$_{0.10}$ at 300 K (found here at 381 and 1021 cm^{-1}), compared with those for LaPO$_4$: Eu$_{0.06}$ (at 380 and 1024 cm^{-1}, are very close to each other.

Finally, comparing the excitation spectrum of KMgLa (PO$_4$)$_2$: Eu^{3+} with that of LaPO$_4$: Eu^{3+} (Fig. 3), we found the Eu^{3+} charge-transfer band (CTB) peaking at 260.5 nm

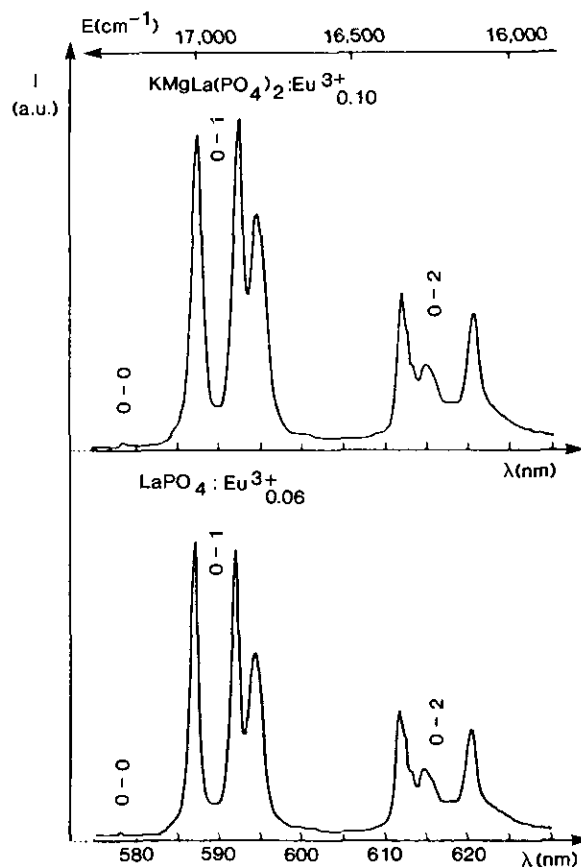FIG. 2. Emission spectra of KMgLa(PO$_4$)$_2$: Eu$_{0.10}^{3+}$ (above) and LaPO$_4$: Eu$_{0.06}^{3+}$ (below) under 267-nm excitation at 300 K, O − *j* (*j* = 0, 1, 2) corresponding to $^5D_0 \rightarrow {}^7F_j$, respectively.

for the former and 259.5 nm for the latter. No striking change occurs in their excitation spectra.

It is necessary to point out that the maxima of CTB and $^5D_0 \rightarrow {}^7F_j$ transitions of LaPO$_4$: Eu^{3+} are different

TABLE 3

$^5D_0 \rightarrow {}^7F_j$ (*j* = 0, 1, 2) Emission Lines of Eu^{3+} in KMgLa(PO$_4$)$_2$ and LaPO$_4$ under a 267-nm Excitation (*T* = 300 K)

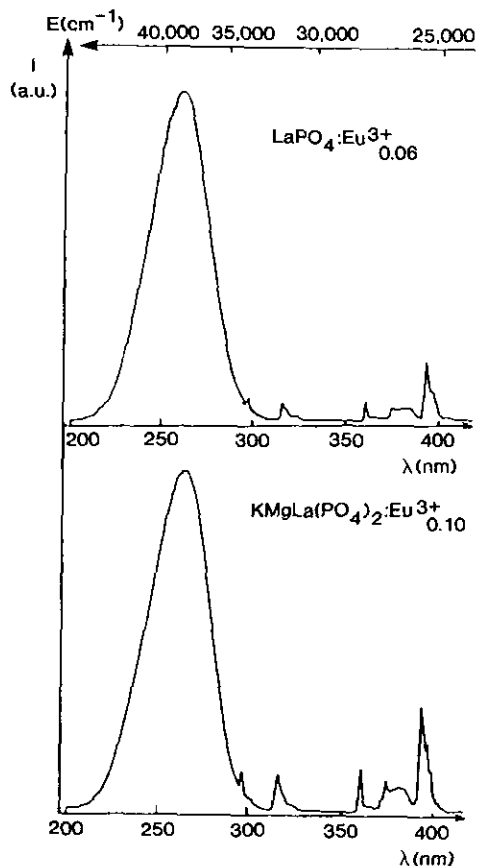| Transitions	KMgLa(PO$_4$)$_2$		LaPO$_4$			
	λ (nm)	E(cm^{-1})	λ (nm)	E(cm^{-1})	E_{exp}[a]	E_{calc}[a]
$^5D_0 \rightarrow {}^7F_0$	578.5 $^5D_0$	17,286	578.1 $^5D_0$	17,298		17,281
$^5D_0 \rightarrow {}^7F_1$	587.5 $^7F_1$	265	587.0 $^7F_1$	262	261	262
	592.5	408	592.0	406	406	411
	594.7	469	594.8	471	464	458
$^5D_0 \rightarrow {}^7F_2$	612.0 $^7F_2$	946	611.7 $^7F_2$	950	943	954
	612.8	967	612.5	971	—	978
	613.5	986	613.3	993	1021	1019
	615.0	1026	614.6	1027	1096	1091
	620.8	1178	620.4	1179	1178	1177

[a] Ref. (6).

FIG. 3. Excitation spectra of $LaPO_4$:$Eu_{0.06}^{3+}$ (above) and $KMgLa(PO_4)_2$:$Eu_{0.10}^{3+}$ (below) with λ_{em} = 592 nm at 300 K.

from those reported in Refs. (10, 11). Our emission spectrum and energy levels for $^7F_1$ and $^7F_2$ on the Eu^{3+} ion in $LaPO_4$, however, are in good agreement with those reported recently by Elisabeth Antic-Fidancev et al. (6).

Based on the accordance of Eu^{3+} spectra in $LaPO_4$ and $KMgLa(PO_4)_2$, we can state that the Eu^{3+} ions in both matrices have the same coordination environment.

CONCLUSION

The crystal structure of $KMgLa(PO_4)_2$ can be deduced from that of monoclinic $LaPO_4$, in which half of the La^{3+} ions are couplingly substituted by K^+ and Mg^{2+} ions with no remarkable change of the lattice. This isomorphous substitution has been confirmed by IR and Eu^{3+}-doped excitation and emission spectra of $KMgLa(PO_4)_2$.

REFERENCES

1. M. Et-Tabirou and A. Daoudi, C. R. Seances Acad. Sci. Ser. C **291**, 93 (1980).
2. L. P. Keller, G. T. McCarthy, and R. G. Garvey, Mater. Res. Bull. **20**, 459 (1985).
3. A. Arbus, C. Duranceau, D. Zambon, and J. C. Cousseins, Eur. J. Solid State Inorg. Chem. **28**, 499 (1991).
4. G. W. Beall, L. A. Boatner, D. F. Mullica, and W. Q. Milligan, J. Inorg. Nucl. Chem. **43**, 101 (1981).
5. D. F. Mullica, W. Q. Milligan, and David A. Grossie, Inorg. Chim. Acta **95**, 231 (1984).
6. Elisabeth Antic-Fidancev, Jorma Hölsä, Michelle Lemaitre-Blaise, and Pierre Porcher, J. Phys. Condens. Matter **3**, 6829 (1991).
7. N. Howell Furman (Ed.), "Standard Methods of Chemical Analysis," 6th ed., Vol. 1, pp. 814, 1064. Van Nostrand, Princeton, NJ, 1962.
8. A. T. Aldred, Acta Crystallogr. Sect. B **40**, 569 (1984).
9. A. Hezel and S. D. Ross, Spectrochim. Acta **22**, 1949 (1966).
10. R. C. Ropp, J. Electrochem. Soc. **115**, 841 (1968).
11. G. Blasse, J. Solid State Chem. **4**, 52 (1972).